ORIGINAL RESEARCH

Inducible Overexpression of GLUT1 Prevents Mitochondrial Dysfunction and Attenuates Structural Remodeling in Pressure Overload but Does Not Prevent Left Ventricular Dysfunction

Renata O. Pereira, PhD; Adam R. Wende, PhD; Curtis Olsen, MS; Jamie Soto, BS; Tenley Rawlings, BS; Yi Zhu, PhD; Steven M. Anderson, PhD; E. Dale Abel, MBBS, DPhil

***Background*—**Increased glucose transporter 1 (GLUT1) expression and glucose utilization that accompany pressure overload-induced hypertrophy (POH) are believed to be cardioprotective. Moreover, it has been shown that lifelong transgenic overexpression of GLUT1 in the heart prevents cardiac dysfunction after aortic constriction. The relevance of this model to clinical practice is unclear because of the life-long duration of increased glucose metabolism. Therefore, we sought to determine if a short-term increase in GLUT1-mediated myocardial glucose uptake would still confer cardioprotection if overexpression occurred at the onset of POH.

***Methods and Results*—**Mice with cardiomyocyte-specific inducible overexpression of a hemagglutinin (HA)-tagged GLUT1 transgene (G1HA) and their controls (Cont) were subjected to transverse aortic constriction (TAC) 2 days after transgene induction with doxycycline (DOX). Analysis was performed 4 weeks after TAC. Mitochondrial function, adenosine triphosphate (ATP) synthesis, and mRNA expression of oxidative phosphorylation (OXPHOS) genes were reduced in Cont mice, but were maintained in concert with increased glucose utilization in G1HA following TAC. Despite attenuated adverse remodeling in G1HA relative to control TAC mice, cardiac hypertrophy was exacerbated in these mice, and positive dP/dt (in vivo) and cardiac power (ex vivo) were equivalently decreased in Cont and G1HA TAC mice compared to shams, consistent with left ventricular dysfunction. O-GlcNAcylation of Ca^{2+} cycling proteins was increased in G1HA TAC hearts.

***Conclusions*—**Short-term cardiac specific induction of GLUT1 at the onset of POH preserves mitochondrial function and attenuates pathological remodeling, but exacerbates the hypertrophic phenotype and is insufficient to prevent POH-induced cardiac contractile dysfunction, possibly due to impaired calcium cycling. **(*J Am Heart Assoc.* 2013;2:e000301 doi: 10.1161/JAHA.113.000301)**

Key Words: cardiac hypertrophy • contractile function • glucose utilization • mitochondria

To meet its substantial energy requirements, the heart is capable of metabolizing a variety of substrates. Loss of this metabolic flexibility has been proposed to be an important cause of cardiac dysfunction in obesity and diabetes.[1] Under physiological conditions, oxidative metabolism of fatty acids (FA) accounts for more than 50% of myocardial adenosine triphosphate (ATP) production[2]; however, glucose assumes greater importance in many clinically relevant circumstances, such as during pressure overload-induced hypertrophy (POH).[3] Cardiac glucose utilization is mainly regulated by glucose uptake via 2 transporters: glucose transporter 1 (GLUT1) and glucose transporter 4 (GLUT4). GLUT1, which contributes to basal cardiac glucose uptake, is highly expressed in the embryonic heart; however, shortly after birth its levels fall as GLUT4 content increases.[4] Despite the developmental repression of GLUT1 expression, a number of pathophysiological conditions are associated with GLUT1 induction in the heart such as myocardial ischemia[5] and left ventricular (LV) hypertrophy.[6] A role for glucose transport in maintaining cardiac function is supported by studies suggesting that increased glucose utilization that accompanies ischemic preconditioning and cardiac hypertrophy

From the Division of Endocrinology, Metabolism and Diabetes, and Program in Molecular Medicine, University of Utah School of Medicine, Salt Lake City, UT (R.O.P., A.R.W., C.O., J.S., T.R., Y.Z., E.D.A.); and Department of Pathology, University of Colorado School of Medicine, Anshutz Medical Campus, Aurora, CO (S.M.A.).

Accompanying online supplementary materials are available at http://jaha.ahajournals.org/content/2/5/e000301/suppl/DC1

Correspondence to: E. Dale Abel, MBBS, DPhil, Fraternal Order of Eagles Diabetes Research Center and Division of Endocrinology and Metabolism, Roy J. and Lucille A. Carver College of Medicine University of Iowa, 108 CMAB, 451 Newton Road, Iowa City, IA 52242. E-mail dale.abel@hmbg.utah.edu

Received May 30, 2013; accepted August 21, 2013.

confers cardioprotection.[7,8] Moreover, lifelong overexpression of GLUT1 in mouse hearts increases glucose utilization, attenuates the development of contractile dysfunction and improves long-term survival after aortic constriction.[9,10] The long-term overexpression of GLUT1 in the aforementioned studies during prenatal development and into adulthood could result in metabolic and transcriptional reprogramming in the heart that could contribute to the cardioprotective effects observed. A more clinically useful approach to determine whether a short-term increase in myocardial glucose uptake would still confer cardioprotection would be to inducibly increase glucose utilization in the context of a hemodynamic stress such as POH. Although pharmacological approaches exist that may increase myocardial glucose utilization in the short term,[11] it is not clear if potential benefits are secondary to glucose or to independent effects of other agents such as insulin or glucagon-like peptide-1 (GLP-1).[12] Therefore, we generated transgenic mice with doxycycline-inducible overexpression of a hemagglutinin (HA)-tagged GLUT1 transgene (G1HA) and subjected these animals to TAC 2 days after transgene induction.

Mitochondrial oxidative capacity is reduced following POH.[1,13,14] The contribution of increased GLUT1-mediated glucose uptake and utilization to cardiac mitochondrial and metabolic adaptations in the context of POH are incompletely understood. We, therefore, sought to determine if induction of GLUT1 expression in cardiomyocytes immediately prior to transverse aortic constriction (TAC) would preserve cardiac mitochondrial and contractile function. We show that short–term induction of GLUT1 in cardiomyocytes at the onset of POH preserves mitochondrial function and attenuates pathological remodeling but is insufficient to prevent POH-induced cardiac contractile dysfunction. G1HA mice may have impaired signaling of calcium cycling proteins after TAC, as suggested by increased glycosylation of the phosphorylated forms of Ca^{2+}/calmodulin-dependent protein kinases II (CaMKII) and phospholamabn (PLB). Thus, increased glucose utilization may have a detrimental effect on calcium signaling, which could explain in part the contractile dysfunction observed in G1HA mice despite attenuated pathological remodeling and preserved mitochondrial function.

Methods

Animals

Double transgenic mice for HA-tagged GLUT1 under the control of the tetracycline response element promoter (TRE-GLUT1) and the codon optimized tetracycline transactivator under control of the α-myosin heavy chain (MHC-rtTA) were generated (G1HA) in the FVB background. TRE-GLUT1 mice were generated at The University of Colorado Health Science Center. To activate the TRE-GLUT1 transgene, mice were given a single injection of 100 μg of doxycycline (DOX) and maintained on DOX-chow (200 mg/kg; Bio-Serv, Frenchtown, NJ and Research Diet, Inc.). Transgene induction was initiated in 6-week-old mice 2 days prior to TAC and resulted in a 4-fold increase in GLUT1 content in the heart. Both Cont and G1HA mice were injected with DOX and then kept on DOX-chow for 4 weeks. Single transgenic littermates were used as controls. The animals were housed at 22°C with a 12-hour light, 12-hour dark cycle with free access to water and standard chow (composition of the chow is in the supplementary materials). Experiments were performed using exclusively male mice. All mouse experiments were approved by the Institutional Animal Care and Use Committee of the University of Utah.

Isolation of Cardiac Myocytes and Determination of 2-Deoxyglucose Uptake

Insulin-stimulated 2-deoxyglucose (2-DG) uptake was measured in collagenase dissociated adult mouse cardiomyocytes from 10-week-old Cont and G1HA mice 2 days after transgene induction as previously described.[15] See supplementary materials for detailed methods.

Surgeries

TAC was performed at the age of 6 weeks using methods previously described.[16] Animals were euthanized 4 weeks after surgery. See supplementary materials for surgical details.

Mouse Characteristics

Four weeks after TAC, body weights were obtained. Mice were then euthanized and hearts and lungs excised and weighed. Tibiae were also removed and their lengths were measured.

Isolated Working Heart

Cardiac substrate metabolism, LV-developed pressure, cardiac output, cardiac power, oxygen consumption, and cardiac efficiency were measured in isolated working hearts obtained after 4 weeks of TAC as previously described.[15] Hearts were perfused with 5 mmol/L glucose and 0.4 mmol/L palmitate. See supplementary materials for detailed methods.

Metabolomics Analysis

Gas chromatography-mass spectrometry (GC-MS) was used to measure tissue levels of glucose, glucose-1-phosphate, glucose-6-phosphate and lactic acid content of snap-frozen heart tissue isolated from Cont and G1HA mice, 4 weeks

after TAC, using previously described protocols[17] at the University of Utah Metabolomics Core Facility. In detail, heart tissue was homogenized and mixed with 9 times volume of −20°C 90% methanol to achieve a final concentration of 80% methanol. The samples were incubated for 1 h at −20°C followed by centrifugation at 30 000*g* for 10 min to precipitate and remove proteins. The supernatant containing the extracted metabolites was then transferred to fresh disposable tubes and completely dried in vacuo. GC-MS analysis of dried samples was performed with a Waters GCT Premier mass spectrometer (Waters) fitted with an Agilent 6890 gas chromatograph (Agilent Technologies) and a GERSTEL MPS2 autosampler (GERSTEL). Data were collected using MassLynx 4.1 software (Waters). Data analysis for glucose and glucose-6-phosphate was performed using QuanLynx, which identified the analytes and their peak area.

Mitochondrial Function

Left ventricular muscle fibers were dissected from freshly excised hearts and permeabilized with saponin. Respiration and ATP synthesis were measured using palmitoyl-carnitine (20 μmol/L, PC) combined with malate (2 mmol/L), or succinate (5 mmol/L) in the presence of rotenone (10 mmol/L) as substrates.[18] See supplementary materials for details.

Histology

Myocardial fragments were stained by Masson's trichrome for visualization and quantification of fibrotic tissue, endothelin-1 immunostaining for quantification of vascularization index, terminal deoxynucleotidyl transferase mediated dUTP nick end labeling assay (TUNEL) and DAPI stains for quantification of apoptotic cells and Periodic acid-Schiff (PAS) stain for visualization of glycogen granules. Stereological analyses were performed for quantification of fibrotic tissue, vascularization and quantification of myocardial glycogen as described in the supplementary materials.

Transthoracic Echocardiography

Mice were anesthetized with isoflurane and placed in the supine position on a heating pad (37°C). Next, the chest hair was removed with a topical depilatory agent. Two-dimensional guided M-mode images were taken in short and long axis projections using a 13-MHz linear probe (Vivid FiVe, GE Medical Systems). LV dimensions and wall thickness were measured in at least 3 beats from each projection and were then averaged. Fractional shortening (%), ejection fraction (%), stroke volume (μL), cardiac output, and heart rate (beats/min) were calculated as previously described.[16]

Hemodynamic Studies

Heart rate, LV systolic pressure (LVSP), LV end-diastolic pressure (LVEDP), and the maximal rate of pressure change (+dP/dt and −dP/dt) were recorded and analyzed as previously described,[19] following insertion of a micromanometer-tipped pressure catheter (Millar Instruments) that was retrogradely introduced into the LV via the right carotid artery. Detailed methods are summarized in the supplementary materials.

RNA Extraction and Quantitative Real-Time PCR

Total RNA was isolated and reverse transcribed to cDNA, which was quantified by real-time PCR (RT-PCR) as previously described and transcript levels normalized to cyclophilin D.[20] Primer sequences and accession numbers are listed in the Online Supplement.

Western Blot Analysis

Immunoblotting was performed with heart homogenates as described in the Online Supplement.

Wheat Germ Agglutinin Immunoprecipitation

To detect the O-GlcNAcylated forms of sarco/endoplasmic reticulum Ca2+-ATPase (Serca2a) and CamKII 720 μg of myocardial protein in 240 μL of lysis buffer were used in each reaction. Then, 40 μL of agarose-bound wheat germ agglutinin (WGA) beads (Vector laboratories) was added to the samples, and they were incubated overnight. After incubation, the beads were spun down at 2000 rpm for 5 min. The pellet containing beads and pulled down proteins was washed 3 times with PBS, and then mixed with 40 μL of 2× sample buffer, boiled for 5 min, and analyzed by Western blot.

Measurements of Mitochondrial DNA

DNA was extracted from 5 mg of heart tissue and purified with a column-based method using the DNeasy Tissue kit (Qiagen Inc). RT-PCR was performed using an ABI Prism qPCR instrument (Applied Biosystems) in a 384-well plate format with SYBR Green I for detection. Mitochondrial DNA content (D-loop noncoding region: D-LP) was expressed relative to genomic Ndufv1.[21] The following primers were utilized:

Primers: 5′ to 3′
D-LP-fwd: GGTTCTTACTTCAGGGCCATCA
D-LP-rev: GATTAGACCCGATACCATCGAGAT
Ndufv1-fwd: CTTCCCCACTGGCCTCAAG
Ndufv1-rev: CCAAAACCCAGTGATCCAGC

Statistical Analysis

Statistical analysis is described in the Online Supplement. Data are presented as means±SEM. RT-PCR and western blot results are presented as fold change versus Cont sham. A probability value of $P \leq 0.05$ was considered significantly different. Significant differences were determined by *t*-test in the experiments where we compared G1HA mice with age-matched Cont. Two-way analysis of variance (ANOVA) was performed to analyze differences by treatment and genotype when we compared 4 groups (Cont sham, Cont TAC, G1HA sham and G1HA TAC), including a Tukey post-hoc analysis when significant interaction occurred. Data were initially log transformed to normalize the distribution. Statistical calculations were performed using the GraphPad Prism Software (GraphPad Software, Inc).

Results

GLUT1 Overexpression Increases 2-DG Uptake in Cardiomyocytes

Inducible overexpression of GLUT1 was achieved in compound transgenic mice expressing TRE-GLUT1 and MHC-rtTA (G1HA) by DOX injection followed by DOX-chow feeding. Two days after DOX treatment, GLUT1 protein in heart homogenates increased by 4-fold in G1HA mice relative to Cont (Figure 1A). This correlated with increased basal and insulin-stimulated 2-DG uptake in isolated cardiomyocytes indicating successful activation of the transgene at the time TAC surgeries were performed (Figure 1B). TAC increased GLUT1 protein content by 2-fold in whole heart homogenates of Cont TAC relative to Cont sham. GLUT1 protein was 2-fold increased in G1HA sham mice and increased an additional 6-fold in transgenic mice following TAC (Figure 1C and 1D). GLUT4 protein was increased in Cont mice after TAC, but did not change in G1HA mice after TAC (Figure 1C and 1E). GLUT1 mRNA was significantly increased in G1HA sham hearts, and was further increased after TAC. This increase was largely accounted for by induction of the HA-tagged transgene (Figure S1A), possibly due to increased rtTA mRNA expression in G1HA TAC mice relative to other groups (Figure S1B). Relative to Cont sham hearts, mRNA levels of GLUT4 and PDK4 genes were modestly but equivalently increased in G1HA sham and in Cont and transgenic mice following TAC (Figure S1).

Substrate Metabolism in G1HA Hearts Following TAC

Substrate metabolism was determined in isolated working hearts, 4 weeks after sham or TAC surgery. Transgene induction in G1HA mice increased glycolysis relative to Cont shams (Figure 2A). After TAC, glycolysis rates increased in Cont hearts, but no further increase was observed in G1HA mice. Relative to sham Cont, glucose oxidation was increased following sham or TAC surgery in G1HA mice, but was unchanged in Cont TAC (Figure 2B) and palmitate oxidation rates were equivalently reduced in Cont and G1HA hearts following TAC but were unchanged in G1HA sham mice (Figure 2C). Metabolomics analysis showed that tissue content of glucose (Figure 2D) and glucose-6-phosphate (Figure 2E) were significantly increased in G1HA hearts after TAC when compared to Cont shams. Glucose-1-phosphate (Figure 2F) and lactic acid were elevated in both Cont and G1HA mice after TAC, but this increase was exacerbated in G1HA mice (Figure 2G). Myocardial glycogen content was increased in Cont TAC mice, but was further increased in G1HA mice after TAC (Figure 2H).

GLUT1 Overexpression Preserves Mitochondrial Function and ATP Synthesis in the Heart

Mitochondrial function was assessed in Cont and G1HA mice 4 weeks after TAC or sham surgeries in saponin-permeabilized cardiac fibers. PC or succinate (in the presence of rotenone)-supported maximal adenosine diphosphate (ADP)-stimulated mitochondrial oxygen consumption (vADP) and ATP synthesis were reduced in Cont mice following TAC (Figures 3A and 3B). Conversely, in G1HA mice, mitochondrial vADP and ATP synthesis were maintained at levels similar to that of Cont sham mice, regardless of TAC operation (Figures 3A and 3B). Preservation of mitochondrial function was likely independent of an increase in mitochondrial number, given similar levels of mitochondrial DNA (mtDNA) (Figure S2A). AMPK activation, was unchanged following TAC in Cont mice, but was reduced in G1HA TAC mice (Figure S2B). Expression of peroxisome proliferator-activated receptor gamma coactivator 1-α (PGC-1α) was reduced, while medium-chain acyl-CoA dehydrogenase (MCAD) and carnitine palmitoyl transferase 1 (CPT1) were unchanged after TAC in Cont hearts. G1HA mice had preserved mRNA expression of PGC-1α and CPT1 and induction of MCAD relative to Cont sham mice, which was maintained after TAC (Figure 4A). Mitochondrial dysfunction observed in Cont TAC mice was accompanied by a decrease in the mRNA expression of a subset of OXPHOS genes (Figure 4B), which were all significantly increased in G1HA mice, regardless of TAC. Protein content of Complex I and Complex IV was not reduced in Cont TAC mice, but was significantly increased in G1HA mice after TAC (Figure 4C).

GLUT1 Overexpression Attenuates Pathological Remodeling After TAC

POH increased cardiac fibrosis and apoptosis (4-fold increase in TUNEL-positive cells) and reduced capillary density in Cont

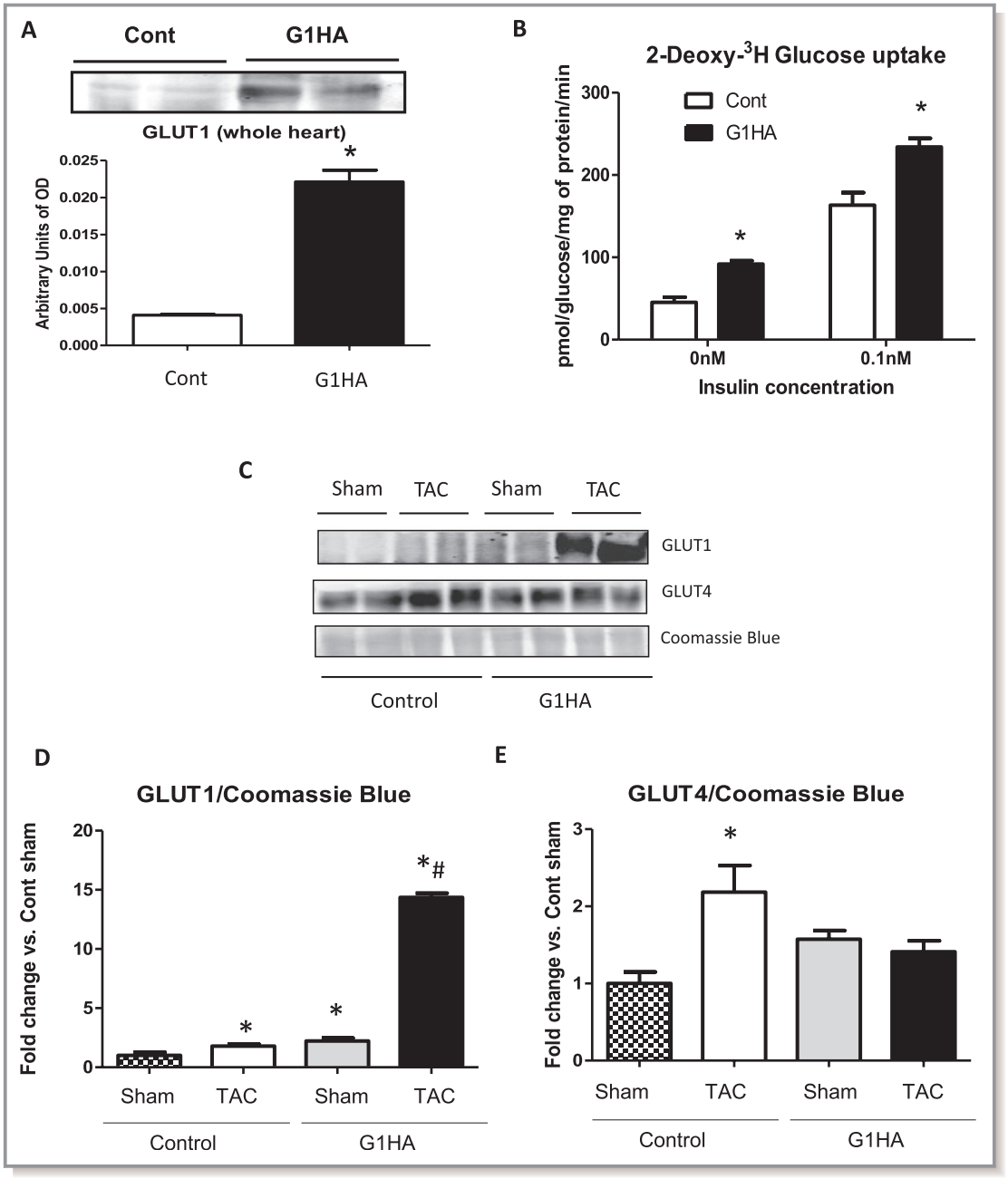

Figure 1. Transgene induction 4 weeks after transverse aortic constriction (TAC). (A) GLUT1 protein content in whole heart homogenates 2 days after DOX injection (mice were 10 weeks at the time of DOX injections). (B) Glucose uptake in isolated cardiomyocytes from Cont and G1HA hearts 2 days after DOX injection. Data are expressed as means±SEM. Significant differences were determined by Student's *t*-test. (*) vs Cont. Two-way ANOVA was performed to analyze differences by treatment and genotype, including a Tukey post hoc analysis when significant interaction occurred. (C) Representative GLUT1 and GLUT4 immunoblot in Cont and G1HA hearts 4 weeks after TAC. (D) Densitometry of GLUT1 protein ($P<0.05$ for genotype and treatment) and (E) densitometry of GLUT4 protein ($P<0.05$ for genotype, treatment, and their interaction). Data are expressed as means±SEM. n=5 mice/group. (*) vs Cont sham (#) vs Cont TAC. Cont indicates control; DOX, doxycycline; G1HA, hemagglutinin-tagged GLUT1 transgene; GLUT1, glucose transporter 1; OD, optical density.

TAC relative to shams (Figure 5A through 5F). In contrast, G1HA mice had a 50% reduction in cardiac fibrotic tissue (Figure 5A and 5B) and an approximate 2-fold decrease in TUNEL-positive cells (Figure 5C and 5D) and reduced Cleaved Caspase 3 protein content (Figure S3) relative to Cont TAC. Vascularization was preserved in G1HA TAC mice relative to Cont TAC (Figure 5 and 5F). To further investigate the mechanisms by which increased GLUT1 expression confers cardioprotection, we analyzed various survival pathways that could be triggered in response to hemodynamic stress. Akt

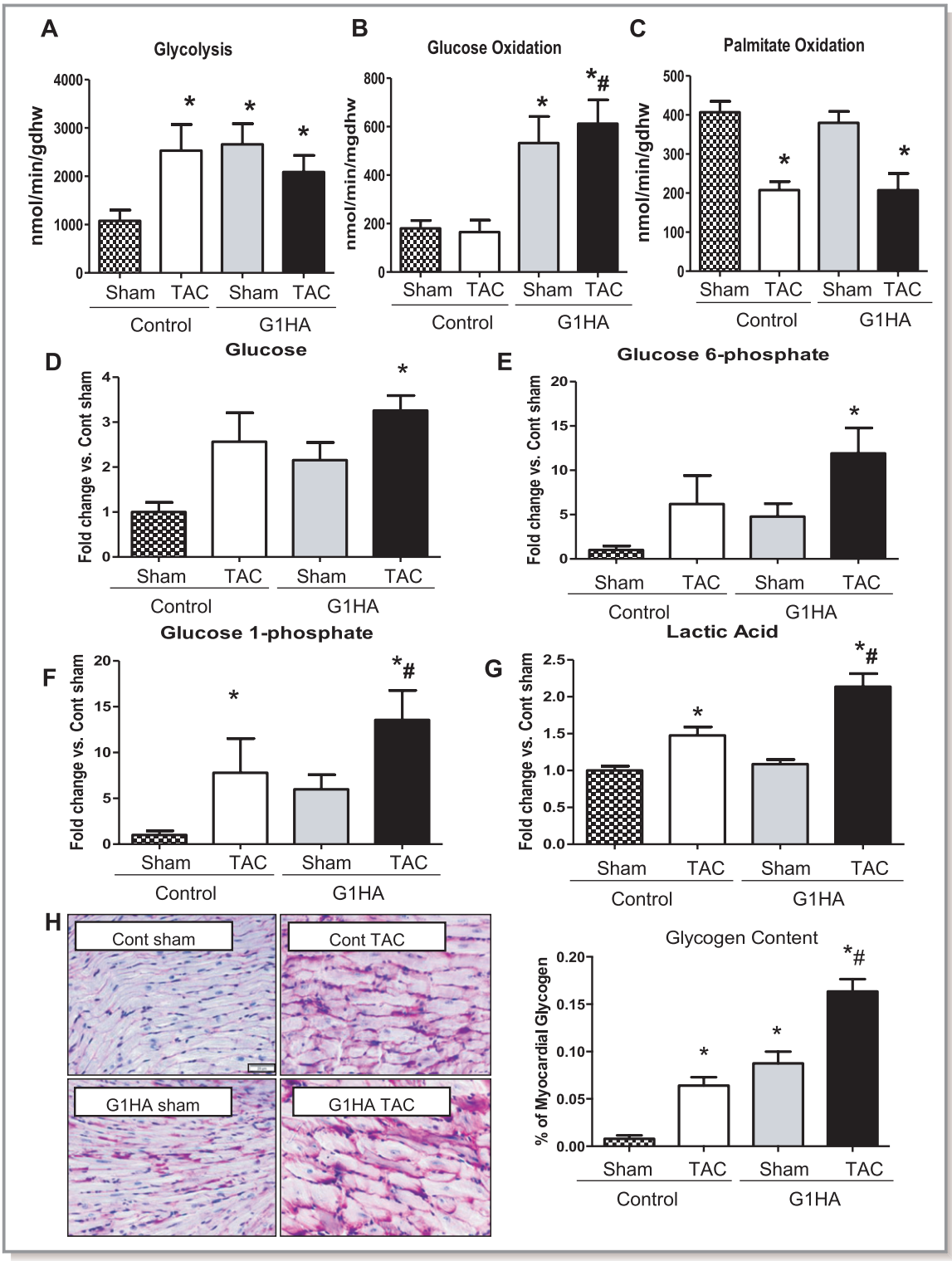

Figure 2. Cardiac substrate metabolism in isolated working hearts and metabolomics (6 hearts per group). Two-way ANOVA was performed to analyze differences by treatment and genotype, including a Tukey post hoc analysis when significant interaction occurred. (A) Glycolysis ($P<0.05$ for genotype and treatment), (B) glucose oxidation ($P<0.05$ for genotype), (C) palmitate oxidation ($P<0.05$ for treatment), (D through G) myocardial tissue levels of glucose ($P<0.05$ for genotype) (D), glucose-6-phosphate ($P<0.05$ for genotype) (E), glucose-1-phosphate ($P<0.05$ for genotype and treatment) (F), lactic acid ($P<0.05$ for genotype and treatment) (G). (H) Myocardial glycogen was evaluated in histological sections stained with periodic acid Schiff (PAS) and percentage of myocardial glycogen quantified (n=4) ($P<0.05$ for genotype, treatment, and their interaction). Data are expressed as means±SEM. (*) vs sham, (#) vs Cont TAC. Cont indicates control; G1HA, hemagglutinin-tagged GLUT1 transgene; GLUT1, glucose transporter 1; TAC, transverse aortic constriction.

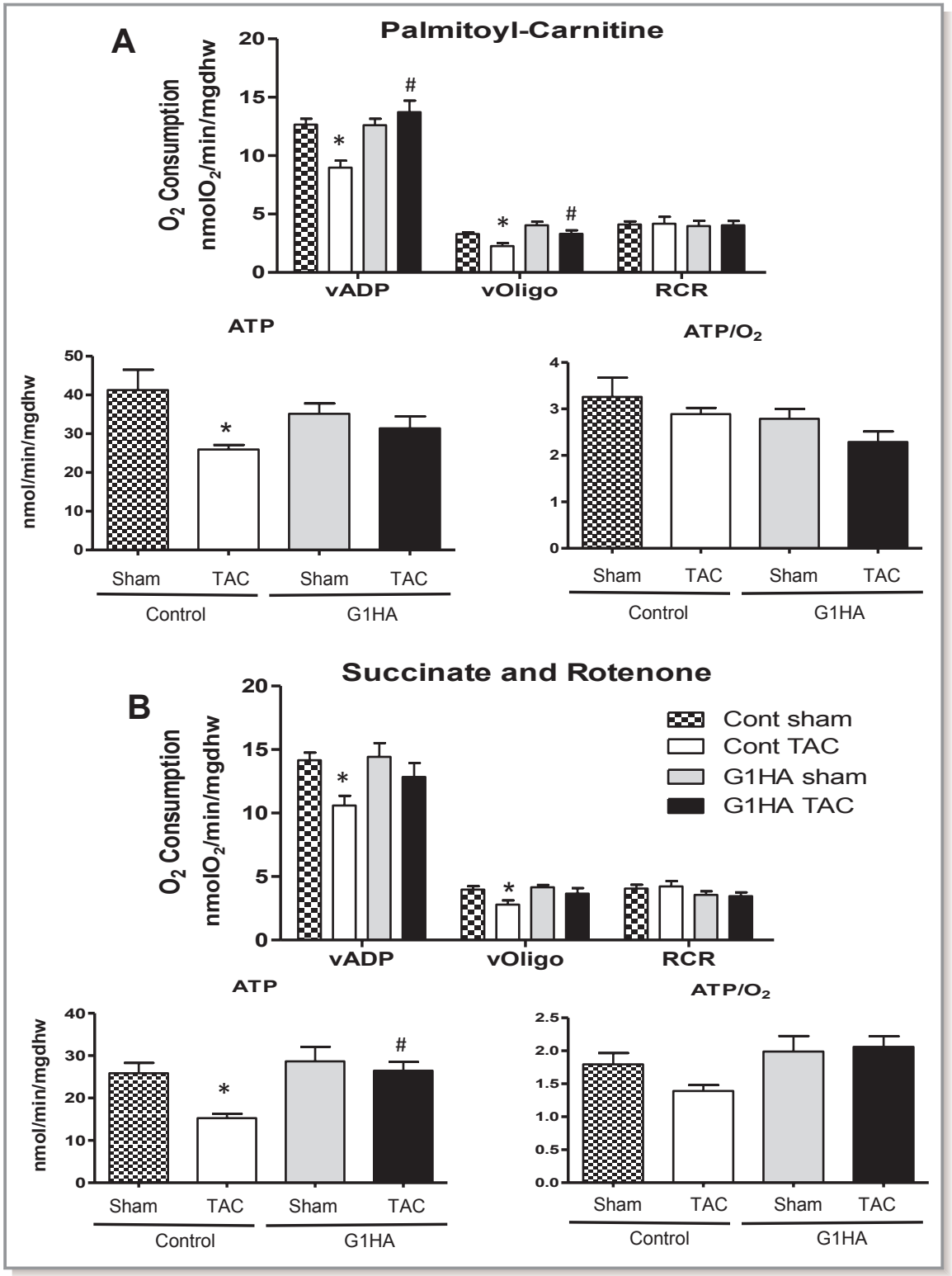

Figure 3. Mitochondrial function is preserved in G1HA mice after TAC (5 to 7 hearts per group). Two-way ANOVA was performed to analyze differences by treatment and genotype, including a Tukey post hoc analysis when significant interaction occurred. Mitochondrial respiration, ATP synthesis rates, and ATP/O ratios were measured in saponin-permeabilized cardiac fibers. (A) Palmitoyl–carnitine (vADP: $P<0.05$ for genotype, treatment, and their interaction; vOligo: $P<0.05$ for genotype and treatment; ATP: $P<0.05$ for treatment) or (B) succinate (in the presence of rotenone) (vADP: $P<0.05$ for treatment; vOligo: $P<0.05$ for treatment; ATP: $P<0.05$ for treatment) were used as substrates. Data are expressed as means±SEM. (*) vs sham, (#) vs Cont TAC. G1HA indicates hemagglutinin-tagged GLUT1 transgene; GLUT1, glucose transporter 1; TAC, transverse aortic constriction.

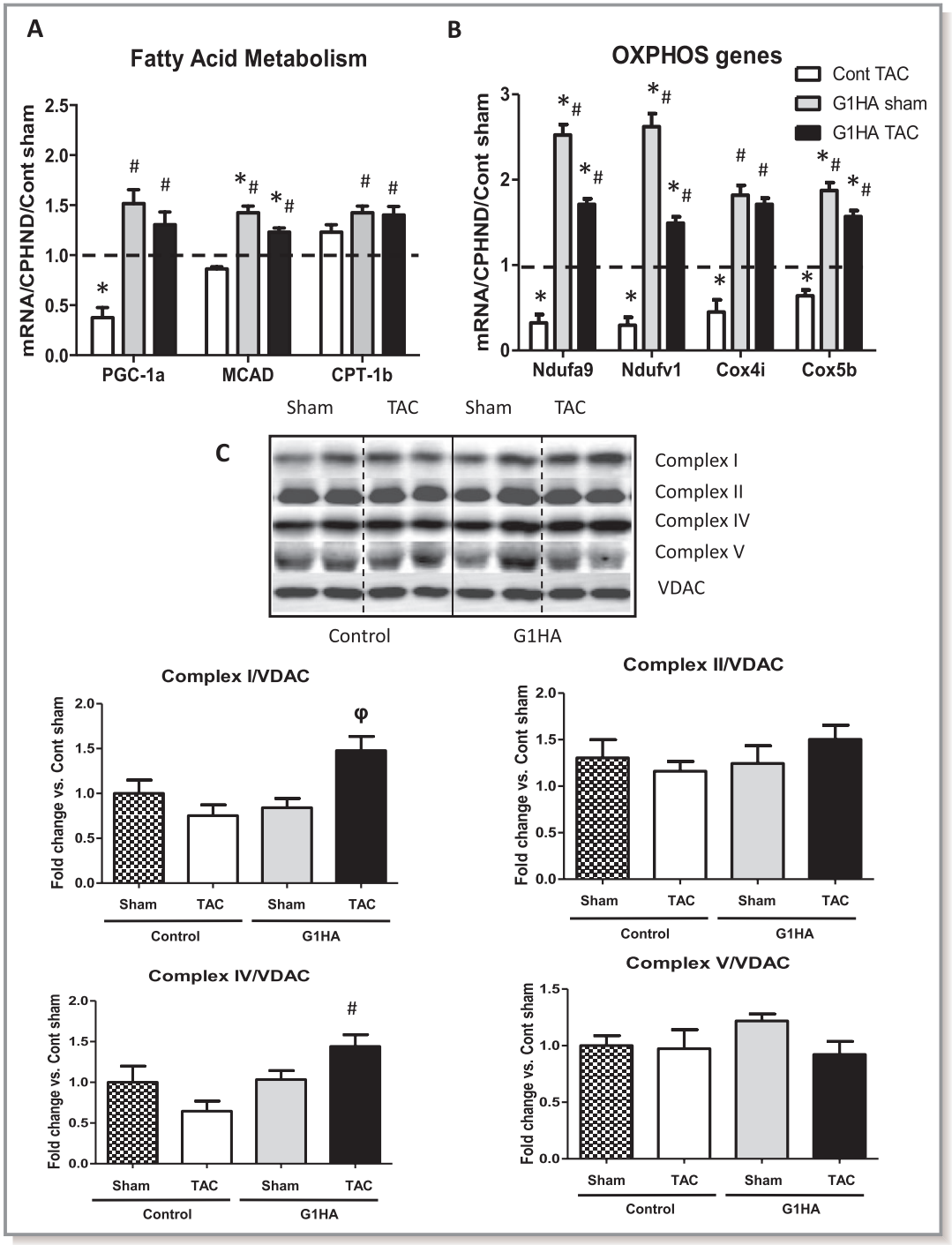

Figure 4. GLUT1 overexpression increases the expression of FAO and OXPHOS genes and proteins after TAC (6 hearts per group). Two-way ANOVA was performed to analyze differences by treatment and genotype, including a Tukey post hoc analysis when significant interaction occurred. (A) Fatty acid oxidation genes (PGC-1α: $P<0.05$ for genotype and treatment; MCAD and CPT-1β: $P<0.05$ for genotype). (B) OXPHOS genes ($P<0.05$ for genotype, treatment, and their interaction), expressed as fold change relative to Cont Sham, which were set as 1 (dashed line). (C) Representative immunoblot of mitochondrial electron transport chain subunits and respective densitometric analysis of protein content normalized to VDAC. Specific proteins probed are: complex I—beta subcomplex 6, subunit 17 kDa ($P<0.05$ for treatment), complex II—iron–sulfur protein, subunit 30 kDa, complex IV—Cox IV, subunit 19.6 kDa ($P<0.05$ for genotype), complex V—F1 complex alpha subunit 59.8 kDa. Data are expressed as means±SEM. (*) vs sham, (#) vs Cont TAC, and (ϕ) vs G1HA sham. Cox indicates cytochrome oxidase; CPHND, cyclophilin D; CPT, carnitine palmitoyl transferase; FAO, fatty acid oxidation; G1HA, hemagglutinin-tagged GLUT1 transgene; GLUT1, glucose transporter 1; MCAD, medium chain acyl CoA dehydrogenase; Ndufa9, NADH dehydrogenase (ubiquinone) 1 alpha subcomplex 9; OXPHOS, oxidative phosphorylation; PGC-1, peroxisome proliferator activated receptor gamma coactivator-1; TAC, transverse aortic constriction; VDAC, voltage dependent anion channel.

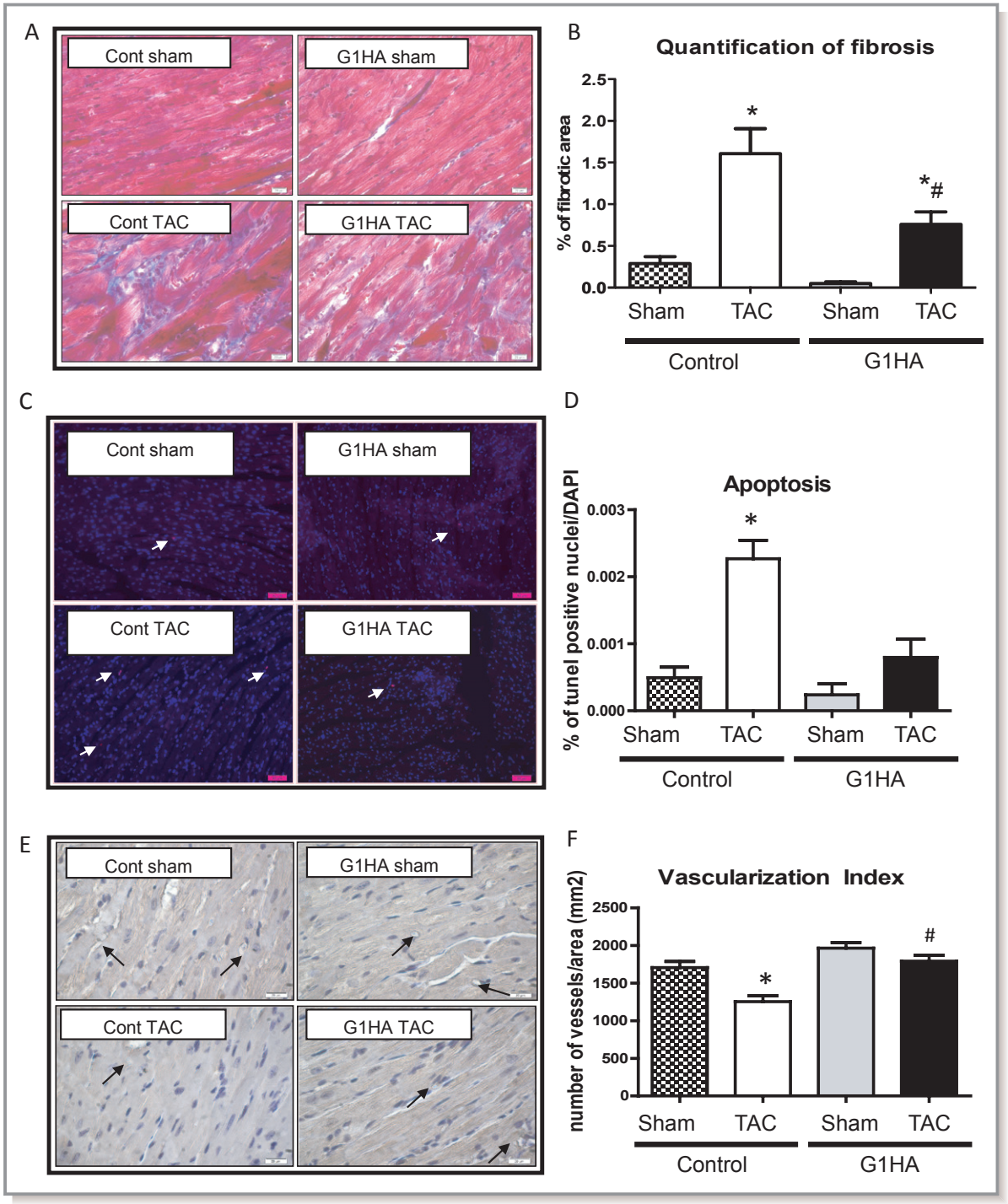

Figure 5. GLUT1 overexpression attenuates pathological remodeling after TAC (5 hearts per group). Two-way ANOVA was performed to analyze differences by treatment and genotype, including a Tukey post hoc analysis when significant interaction occurred. (A) Masson's trichrome staining of heart sections. (B) Quantification of percentage of fibrotic area ($P<0.05$ for genotype and treatment). (C) TUNEL staining. (D) Quantification of % of TUNEL positive nuclei normalized to DAPI staining ($P<0.05$ for genotype). (E) Endothelin 1 staining. (F) Quantification of vascularization ($P<0.05$ for genotype and treatment). Data are expressed as means±SEM. (*) vs sham, (#) vs Cont TAC. Cont indicates control; G1HA, hemagglutinin-tagged GLUT1 transgene; GLUT1, glucose transporter 1; GPX-1, glutathione peroxidase 1; GPX-4, glutathione peroxidase 4; TAC, transverse aortic constriction; TUNEL, terminal deoxynucleotidyl transferase mediated dUTP nick end labeling assay.

was activated similarly in response to TAC in both Cont and G1HA hearts (Figure S4). In contrast, HIF-1α protein content was significantly increased only in transgenic mice following TAC (Figure 6A). In parallel, vascular endothelial growth factor (VEGF) protein content was also induced in G1HA TAC mice relative to Cont mice (Figure 6B). In addition, expression

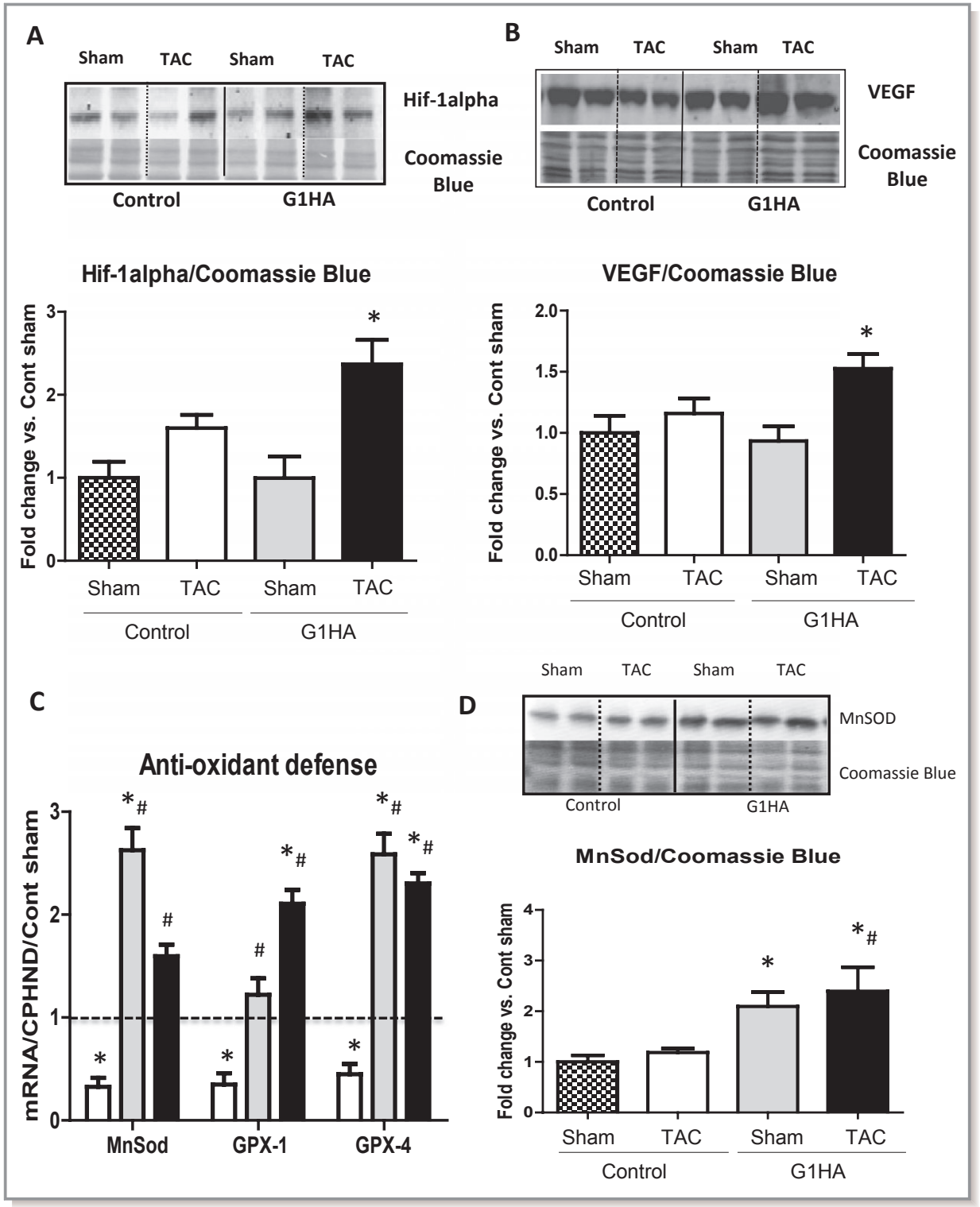

Figure 6. Hif-1α, VEGF, and antioxidant defense proteins are induced in G1HA hearts (5 hearts per group). Two-way ANOVA was performed to analyze differences by treatment and genotype, including a Tukey post hoc analysis when significant interaction occurred. (A) Western blot image and densitometry for HIF-1 alpha protein ($P<0.05$ for genotype). (B) Western blot image and densitometry for VEGF protein ($P<0.05$ for genotype). (C) mRNA expression of genes involved in the antioxidant defense expressed as fold change relative to Cont sham (dashed line) ($P<0.05$ for genotype, treatment, and their interaction). Bar colors correspond to those in (A). (D) Western blot image and densitometry for MnSOD ($P<0.05$ for genotype and treatment). Data are expressed as means±SEM. (*) vs sham, (#) vs Cont TAC. Cont indicates control; G1HA, hemagglutinin-tagged GLUT1 transgene; GLUT1, glucose transporter 1; HIF-1 hypoxia-inducible factor-1; MnSOD, manganese superoxide dismutase; TAC, transverse aortic constriction; VEGF, vascular endothelial growth factor.

levels of genes involved in antioxidant defense, namely manganese superoxide dismutase (MnSOD), glutathione peroxidase 1 (Gpx1) and glutathione peroxidase 4 (Gpx4), were reduced in Cont TAC mice, but were increased or preserved in G1HA mice regardless of TAC surgery (Figure 6C). The protein content of MnSOD was unchanged in Cont TAC mice relative to shams, but was significantly higher in G1HA mice and this increase was maintained after 4 weeks of TAC (Figure 6D).

Increased GLUT1-mediated Glucose Uptake Does Not Prevent Contractile Dysfunction and Exacerbates the Hypertrophic Phenotype

Aortic pressure was reduced in the Cont and G1HA mice following TAC (Figure 7A). Cardiac power (Figure 7B), cardiac output (Figure 7C), oxygen consumption (Figure 7D), and cardiac efficiency (Figure 7E) declined equivalently in TAC mice of both genotypes. LV wall dimensions were equivalently increased in both Cont and G1HA mice following TAC. In contrast, ejection fraction and fractional shortening were reduced in Cont TAC mice, but were unchanged in G1HA TAC mice relative to sham-operated mice (Table 1). However, LV catheterization revealed similar increases in LVEDP and LVDevP and equivalent reductions in peak rates of ventricular contraction (+dP/dt) following TAC in Cont and G1HA, respectively (Table 2). Interestingly, isovolumic relaxation constant (Tau) was significantly increased in G1HA mice relative to all groups (Table 2), indicating abnormal diastolic function in these mice. mRNA expression of the hypertrophy markers atrial natriuretic peptide (ANP), B-type natriuretic peptide (BNP), actin, alpha skeletal muscle (ACTA1), and β-myosin heavy chain (β-MHC) were increased with TAC in both genotypes, but ANP and β-MHC were induced to a greater extent in G1HA hearts relative to Cont (Figure 7F). GLUT1 overexpression did not induce hypertrophy at base line. Following TAC, G1HA mice exhibited significantly more hypertrophy relative to Cont TAC, as evidenced by increased heart weight to tibia length ratios (Figure 7G). Wet lung weight to tibia length ratios were equivalently increased in Cont and G1HA mice following TAC, indicating similar degrees of pulmonary edema resulting from LV dysfunction (Figure 7H). Body weight was significantly decreased in G1HA mice 4 weeks after TAC, but tibia length measurements were unchanged between groups (Table S1).

GLUT1 Overexpression Increases *O*-GlcNAc Modification of Calcium Cycling Proteins Following TAC

GLUT1 overexpression attenuates LV remodeling and preserves mitochondrial function, but does not improve cardiac contractility. We, therefore, examined potential mechanisms by which increased glucose utilization might impair cardiac function despite obvious structural and metabolic benefits. Serca2a mRNA expression was repressed by TAC in Cont and G1HA mice, despite baseline induction in G1HA sham hearts, and CaMKII mRNA expression was significantly increased in G1HA mice after TAC relative to all groups (Figure S5A). Protein content of Serca2a, CaMKII and phospholamban (PLB) were unchanged between groups, but phosphorylation of CaMKII and PLB was increased in G1HA TAC relative to Cont sham mice (Figure S5B). *O*-GlcNAcylation of calcium cycling proteins has been correlated with LV dysfunction in various cardiomyopathies.[22,23] We observed an overall increase in *O*-GlcNAcylation of myocardial proteins in G1HA TAC mice relative to Cont TAC (Figure 8A). Immunoprecipitation of glycosylated proteins, followed by immunoblot for calcium cycling proteins revealed increased *O*-GlcNAcylation of the phosphorylated forms of CaMKII and PLB proteins in G1HA mice following TAC (Figure 8B). It has been recently suggested that glucose-6-phosphate plays a critical role in load-induced mTOR activation leading to endoplasmic reticulum stress, and contractile dysfunction.[24] Given the increased glucose-6-phosphate in hearts of G1HA mice following TAC, we determined S6 phosphorylation as an index of mTOR activation. S6 phosphorylation was significantly increased in G1HA mice following TAC, relative to Cont and G1HA sham hearts (Figure S6).

Discussion

Increased glucose uptake and glycolysis have been consistently observed in hypertrophied hearts.[25–28] Although the functional significance of this adaptation is not completely understood, this increase in glucose utilization is believed to be cardioprotective.[29] Previous studies using transgenic mice with lifelong cardiac-specific overexpression of GLUT1 demonstrated that long-term increases in basal glucose uptake and glycolysis in adult mouse hearts confer increased tolerance to chronic pressure overload and delays the progression to heart failure following ascending aortic constriction.[9] It is unclear though, due to the embryonic onset of increased GLUT1 overexpression, if the cardioprotective effects observed are a direct result of increased glucose uptake or an indirect effect due to metabolic and transcriptional reprogramming in the heart. Therefore, in the present study, we utilized a more clinically relevant model in which short-term inducible GLUT1 overexpression was used to investigate if a cardiomyocyte-specific increase in GLUT1-mediated glucose uptake shortly prior to POH would still confer cardioprotection. Our study reports that in contrast to models with lifelong cardiac GLUT1 overexpression, short-term induction of GLUT1 in cardiomyocytes is not

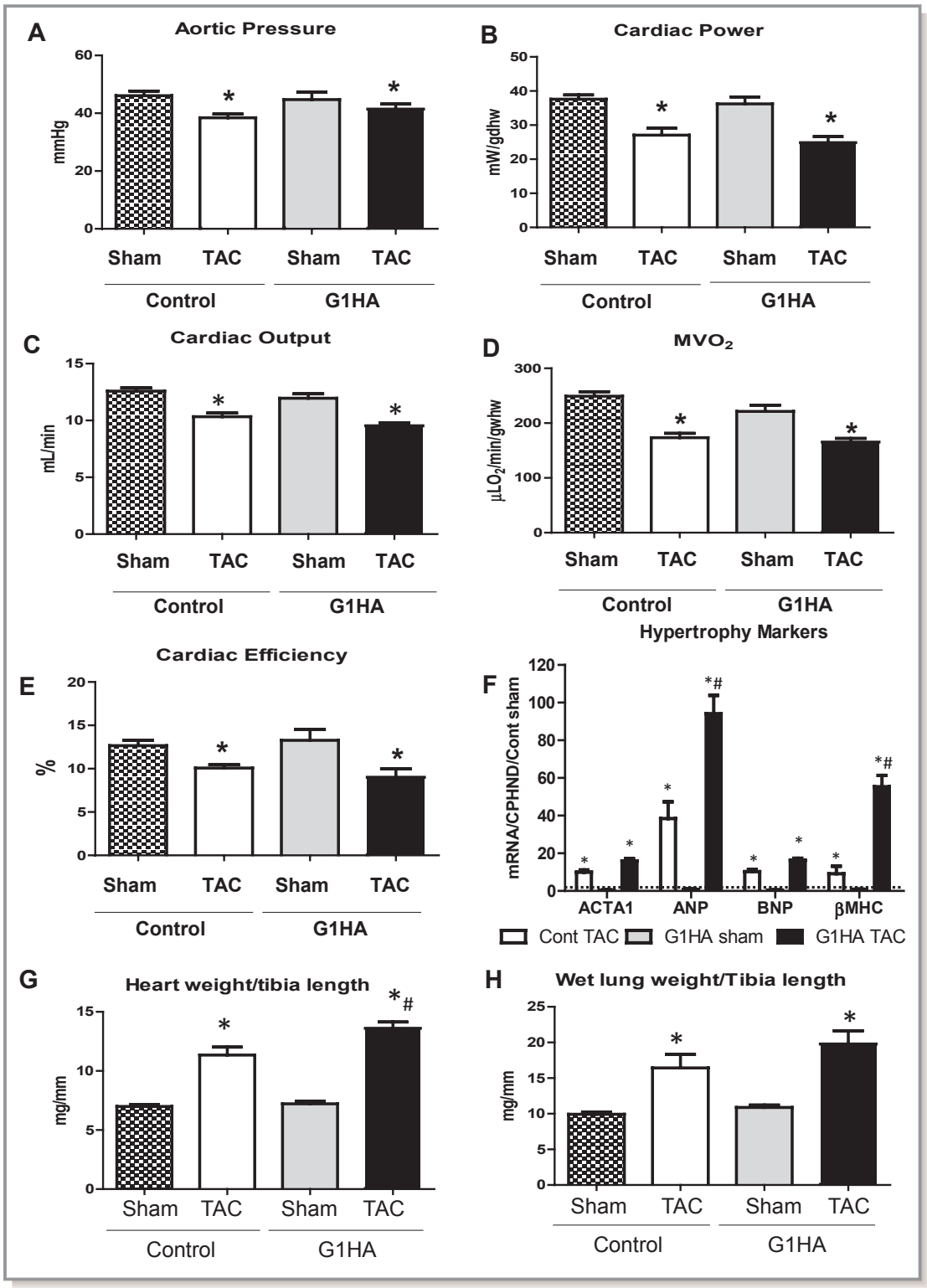

Figure 7. Cardiac function in isolated working hearts and cardiac hypertrophy following TAC. Two-way ANOVA was performed to analyze differences by treatment and genotype, including a Tukey post hoc analysis when significant interaction occurred. (A) Aortic pressure ($P<0.05$ for treatment), (B) cardiac power ($P<0.05$ for treatment), (C) cardiac output ($P<0.05$ for treatment), (D) oxygen consumption (MVO_2) ($P<0.05$ for treatment), and (E) cardiac efficiency ($P<0.05$ for treatment). (F) mRNA expression of hypertrophy markers (ACTA1 and BNP: $P<0.05$ for treatment; ANP and β-MHC: $P<0.05$ for genotype and treatment), (G) heart weight to tibia length ratios ($P<0.05$ for genotype and treatment) and (H) lung weight to tibia length ratios ($P<0.05$ for treatment) in Cont and G1HA hearts 4 weeks after TAC. Data are expressed as means±SEM. (*) vs sham, (#) vs Cont TAC. ANP indicates atrial natriuretic peptide; BNP, B-type natriuretic peptide; G1HA, hemagglutinin-tagged GLUT1 transgene; GLUT1, glucose transporter 1; MHC, myosin heavy chain; TAC, transverse aortic constriction.

Table 1. Echocardiography

	Cont Sham (n=5)	Cont TAC (n=5)	G1HA Sham (n=5)	G1HA TAC (n=5)
Ejection fraction, %	72.75±0.44	64.12±4.34*	70.32±1.17	70.21±2.60
Fractional shortening, %	35.18±0.35	28.24±3.17*	33.37±0.87	33.45±1.99
Stroke volume, mL	0.045±0.002	0.045±0.002	0.051±0.003	0.051±0.002
Heart rate, bpm	501±20	446±40	499±11	372±13*†
IVSs, cm	0.142±0.003	0.150±0.014	0.145±0.004	0.172±0.009*
IVSd, cm	0.096±0.003	0.111±0.008	0.010±0.004	0.123±0.005*
LVIDs, cm	0.250±0.003	0.271±0.014	0.274±0.010	0.273±0.016
LVIDd, cm	0.389±0.006	0.391±0.007	0.411±0.012	0.410±0.016
LVPWs, cm	0.117±0.003	0.137±0.007*	0.116±0.003	0.142±0.008*
LVPWd, cm	0.087±0.003	0.103±0.005*	0.086±0.002	0.101±0.006*

Two-way ANOVA was performed to analyze differences by treatment and genotype, including a Tukey post hoc analysis when significant interaction occurred. Data are expressed as means±SEM. Ejection fraction and fractional shortening ($P<0.05$ for treatment). Heart rate ($P<0.05$ for genotype and treatment). Cont indicates control; G1HA, hemagglutinin-tagged GLUT1 transgene; IVSd, interventricular septum in diastole and IVSs, interventricular septum in systole ($P<0.05$ for genotype and treatment); LVIDd, left ventricle internal diameter in diastole; LVIDs, left ventricle internal diameter in systole; LVPWd, left ventricle posterior wall in diastole and LVPWs, left ventricle posterior wall in systole $P<0.05$ for treatment); TAC, transverse aortic constriction.

*$P<0.05$ compared to sham.

†$P<0.05$ compared to Cont TAC.

sufficient to prevent LV contractile dysfunction if it occurs at the onset of POH, despite beneficial effects on mitochondrial, metabolic and structural remodeling. Here, we suggest that one possible mechanism underlying the impaired contractility observed in G1HA mice after TAC is increased *O*-GlcNAcylation of calcium cycling proteins.

G1HA TAC exhibited an approximate 15-fold increase in GLUT1 content versus a 4-fold increase observed in G1HA sham relative to Cont sham mice. This additional increase in GLUT1 was likely due to further activation of the transgene following TAC, as evidenced by increased HA-tagged GLUT1 mRNA expression relative to sham mice. Indeed, rtTA mRNA levels were elevated in G1HA mice, but not in Cont mice following TAC. The mechanisms underlying this increase are not completely elucidated in the present study, but the possibility exists that TAC induced the activation of the MHC-rtTA transgene in G1HA mice, which might have contributed to the further induction of the GLUT1 transgene. Hif-1 α, a transcription factor known to induce GLUT1 expression, was elevated in G1HA mice after TAC, which could also have contributed to the further increase in GLUT1 in these mice. It is noteworthy that the additional increase in GLUT1 content in G1HA TAC mice did not further increase myocardial glucose content, rates of glycolysis or glucose oxidation relative to G1HA sham mice, or glycolysis rates relative to Cont TAC. This may suggest that other steps in glycolysis could be rate limiting for glycolysis induction in pressure overload or that the additional transgene induction

Table 2. Left Ventricle Catheterization

	Cont Sham (n=7)	Cont TAC (n=7)	G1HA Sham (n=7)	G1HA TAC (n=7)
+dP/dt, mm Hg/s	9311±521	6638±384*	8810±453	5501±545*†
−dP/dt, mm Hg/s	−7531±566	−8180±514	−6764±412.1	−7361±762.3
LVDevP, mm Hg	97.4±4.5	145.6±6.5*	94.8±4.3	144.4±6.2*
LVEDP, mm Hg	9.7±1.7	24.3±5.0*	16.9±2.3	33.4±4.0*
Heart rate, bpm	441±16	437±16	442±8	414±19
Tau, ms	15.12±1.3	17.47±1.5	18.14±1.9	31.02±5.0*†

Two-way ANOVA was performed to analyze differences by treatment and genotype, including a Tukey post hoc analysis when significant interaction occurred. Data are expressed as means±SEM. Cont indicates control; +dP/dt, rate of rise of left ventricular pressure ($P<0.05$ for genotype and treatment) and −dP/dt, rate of fall of left ventricular pressure; G1HA, hemagglutinin-tagged GLUT1 transgene; LVDevP, left ventricular developed pressure and LVEDP, left ventricular end diastolic pressure ($P<0.05$ for treatment); TAC, transverse aortic constriction; Tau, isovolumic relaxation constant ($P<0.05$ for genotype and treatment).

*$P<0.05$ compared to sham.

†$P<0.05$ compared to Cont TAC.

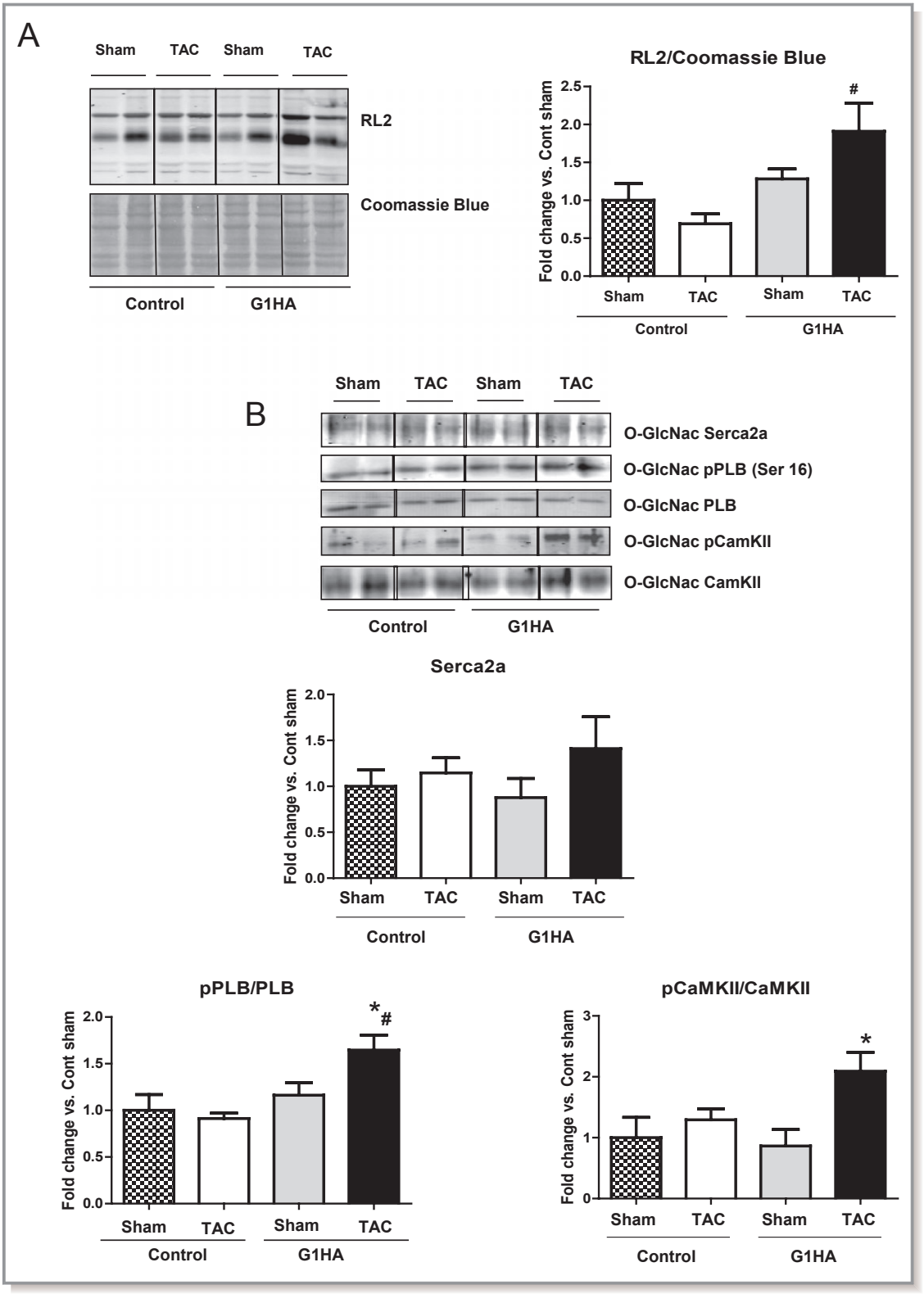

Figure 8. *O*-GlcNAcylation of calcium cycling proteins. Two-way ANOVA was performed to analyze differences by treatment and genotype, including a Tukey post hoc analysis when significant interaction occurred. (A) Western blot and densitometry for RL2 in Cont and G1HA mice after TAC ($P<0.05$ for genotype). (B) Immunoblots and densitometry for the following *O*-GlcNAcylated proteins: Serca2a normalized to the input, total and phosphorylated PLB ($P<0.05$ for genotype and treatment) and total and phosphorylated CaMKII ($P<0.05$ for treatment) (n=6). Data are expressed as means±SEM. (*) vs sham, (#) vs Cont TAC. CaMKII indicates Ca^{2+}/calmodulin-dependent protein kinases II; G1HA, hemagglutinin-tagged GLUT1 transgene; GLUT1, glucose transporter 1; PLB, phospholamabn; TAC, transverse aortic constriction.

increases the flux of glucose carbons into alternative pathways such as the pentose phosphate and hexosamine biosynthetic pathways. Interestingly, glucose-6-phosphate, a precursor for both pathways, and glucose-1-phosphate, a precursor for glycogen synthesis were significantly increased only in G1HA TAC mice when compared to Cont shams. Consistently, myocardial glycogen content was also significantly increased in G1HA TAC mice, when compared to the other groups. Elevated *O*-GlcNAcylation of myocardial proteins in G1HA TAC mice further supports a possible increase in the flux of glucose carbons into the hexosamine biosynthetic pathway. Taken together, these data are consistent with increased glucose uptake in G1HA TAC mice and potentially increased flux through these alternative pathways.

It is widely accepted that mitochondrial dysfunction develops in pathological cardiac hypertrophy.[30] Consistent with this notion, Cont TAC mice had impaired mitochondrial function and reduced ATP production as demonstrated by reduced vADP, when 2 different substrates were used. Mitochondrial dysfunction in Cont TAC mice was observed concomitantly with reduced expression of OXPHOS genes. Conversely, G1HA mice had preserved mitochondrial function and ATP synthesis following TAC, which was accompanied by increased expression of a subset of OXPHOS genes and higher levels of PGC-1α and MCAD genes. Because mtDNA was unchanged between groups, we believe that the mitochondrial phenotype observed in transgenic hearts is not related to changes in mitochondrial number, but rather to PGC-1α-mediated changes in the transcriptional machinery that sustains mitochondrial oxidative capacity in adult myocytes. G1HA mice exhibit impaired contractile dysfunction despite normal mitochondrial function. These data suggest that mitochondrial dysfunction per se might not mediate the transition from compensated cardiac hypertrophy to heart failure, but when it occurs is secondary to other pathophysiological processes that drive this transition. These data also suggest that contractile dysfunction in pressure overload-induced hypertrophy may occur independently of mitochondrial dysfunction. The present study suggests that GLUT1-mediated glucose utilization may stimulate transcriptional networks such as PGC-1α, via mechanisms that remain to be elucidated, that increase mitochondrial oxidative capacity. These observations support conserved and coordinated glucose regulated prosurvival pathways that may limit LV remodeling in pressure overload-induced cardiac hypertrophy.

Pathological remodeling was attenuated in G1HA hearts following TAC, as evidenced by reduced fibrosis, decreased apoptosis and preserved capillary density. Increased GLUT1 or increased glucose uptake have been implicated in cellular protection and survival.[31] GLUT1 overexpression in cardiomyocytes and vascular smooth muscle cells decreases apoptosis in response to hypoxic stress,[32,33] or serum deprivation.[34] Thus, we sought to determine if the cardioprotective effects conferred by GLUT1 resulted from the activation of prosurvival signaling pathways and/or antioxidant defense. Increased Akt signaling, which is observed in cardiac hypertrophy,[35] was equivalently induced in Cont and G1HA mice upon POH, suggesting that the GLUT1-mediated cardioprotection is independent of Akt. In contrast, TAC resulted in a 2-fold increase in Hif-1α protein content in G1HA mice, which correlated with increased VEGF levels in these hearts. A critical role for Hif-1α in POH has been suggested by studies in mice with conditional deletion of Hif-1α, which manifest rapid cardiac decompensation accompanied by increased myocardial hypoxia, apoptosis, cardiac fibrosis, myocardial hypertrophy and decreased myocardial capillary density following TAC.[36] Studies in tumor cells suggest that pyruvate and lactic acid arising from increased glycolysis can induce HIF-1α expression, suggesting the existence of a feed-forward mechanism, in which induction of HIF-1 increases pyruvate/lactate, which in turn further augments HIF-1 activity.[37,38] Tissue content of lactate was further increased in G1HA mice relative to Cont after TAC, which offers a plausible mechanism by which Hif-1α was induced in these mice. Because myocardial oxidative stress has been implicated in the transition from compensated hypertrophy to heart failure,[39,40] we investigated the expression of genes involved in antioxidant defense in the hearts of Cont and G1HA mice following TAC. mRNA expression levels of MnSOD, GPX-1 and GPX-4 were reduced in Cont TAC mice, whereas these genes were induced in nonstressed G1HA mice relative to Cont and were maintained after TAC. Additionally, MnSOD protein content was increased in G1HA mice regardless of TAC surgery, suggesting that decreased oxidative stress represents a possible mechanism for the attenuated pathological remodeling in G1HA mice. Additional studies need to be performed in the future to precisely elucidate the mechanisms by which glucose regulates the expression of these antioxidant genes. This study suggests, though, that 2 possibilities could be induction of MnSOD by HIF,[41] or by PGC-1α.[42]

Despite the beneficial effects of GLUT1 overexpression at the onset of POH on metabolic, mitochondrial and structural remodeling in G1HA, our findings suggest that GLUT1-mediated glucose uptake might amplify the hypertrophic response to TAC without increasing LV contractility. Phosphorylation of CaMKII on Threonine 286 residues and PLB on serine 16 residues was significantly increased in G1HA mice after TAC. These changes have been recently shown to contribute to the development of heart failure.[43,44] Some indices of contractile function were impaired to a greater extent in G1HA mice following TAC, as exemplified by the higher Tau. Thus, although increased glucose utilization may confer cardioprotective effects, excessive glucose uptake might be detrimental to cardiac contractility. Ca^{2+} cycling, a key mechanism that

modulates contractile force generation, contributes mechanistically to myocardial contractile dysfunction in heart failure.[45,46] Exposing cardiac myocytes to high glucose or elevated glucosamine (a precursor of *O*-GlcNAc) reduced contractility and calcium transients in these cells.[47] Moreover, in vivo studies in mice demonstrated that LV dysfunction in a model of diabetic cardiomyopathy was associated with excess protein *O*-GlcNAcylation. Reversing excessive *O*-GlcNAc modification by overexpressing an adenovirus-encoded *O*-GlcNAcase enzyme in the heart restored cardiac function in STZ-induced diabetes, which was correlated with increased phosphorylation of PLB and enhanced Serca2a function.[22] In the present study, increased GLUT1-mediated glucose uptake led to increased protein *O*-GlcNAcylation following TAC. Interestingly, we observed increased *O*-GlcNAcylation of the phosphorylated forms of CaMKII and PLB in G1HA TAC hearts. Although the functional significance of our findings is not clear, the possibility exists that increased *O*-GlcNAcylation of calcium cycling proteins might have detrimental effects on contractile function in G1HA TAC hearts. Further studies are needed to determine if reversing the increase in *O*-GlcNAcylation in our model is enough to normalize contractile function, and to identify the exact mechanisms by which excess glucose may impair calcium cycling in these hearts. Moreover, increased glucose-6-phosphate levels and activation of mTOR signaling might contribute to the impaired contractile function observed in G1HA TAC mice, as was recently suggested.[24]

In summary, the present study identifies a role for short-term induction of GLUT1 in maintaining mitochondrial function, increasing the expression of OXPHOS genes and in preventing cell death and cardiac fibrosis by mechanisms that may involve the activation of Hif-1α and preservation of antioxidant defenses. Despite these beneficial effects of GLUT1 overexpression in attenuating adverse structural and mitochondrial remodeling, they were insufficient to maintain contractile function in hearts subjected to POH. These data importantly illustrate that normalization of mitochondrial function and increased glucose metabolism can be dissociated from an improvement in contractile function following transverse aortic constriction. We provide evidence that suggests excess glucose might have a short-term detrimental effect on calcium signaling in G1HA TAC mice, which could represent a potential mechanism leading to impaired contractile function. Thus, short-term induction of glucose utilization in the context of POH is a double-edged sword in which attenuation of structural and mitochondrial remodeling is offset by glucose-dependent mechanisms that limit contractility. Whether or not the mitochondrial and structural benefits will lead to more rapid restoration of cardiac function if pressure overload is ameliorated remains an important question for future study. Our study also has important clinical implications. It has been reported that as cardiac hypertrophy progresses to heart failure, GLUT1 mRNA expression is repressed in human hearts, suggesting that decreased GLUT1-mediated glucose uptake and utilization could contribute to the transition to heart failure.[48,49] Therefore, therapeutic strategies that maintain glucose utilization could potentially be utilized to retard or prevent the transition to heart failure in humans. However, further studies are needed to determine the optimal level of glucose utilization, given the potential detrimental effects of excessive glucose availability on contractile function.

Acknowledgments

The authors thank Jeffrey Lei, Sylvia Hu, and Li Wang for important technical help during the course of these studies.

Sources of Funding

These studies were supported by National Institute of Health (NIH) grant RO1DK092065 and U01 HL087947 to E.D.A. who is an established investigator of the American Heart Association and PO1 HD 038129 and RO1 CA 138482 to Dr Anderson.; Dr Pereira was supported by a postdoctoral fellowship from the American Heart Association (AHA) Western Affiliates and NIH Grant 5T32 HL007576. Dr Wende was supported by an advanced postdoctoral fellowship from the JDRF and a postdoctoral fellowship from the AHA Western Affiliates.

Disclosures

None.

References

1. Huss JM, Kelly DP. Mitochondrial energy metabolism in heart failure: a question of balance. *J Clin Invest*. 2005;115:547–555.
2. Taegtmeyer H. Energy metabolism of the heart: from basic concepts to clinical applications. *Curr Probl Cardiol*. 1994;19:59–113.
3. Nascimben L, Friedrich J, Liao R, Pauletto P, Pessina AC, Ingwall JS. Enalapril treatment increases cardiac performance and energy reserve via the creatine kinase reaction in myocardium of syrian myopathic hamsters with advanced heart failure. *Circulation*. 1995;91:1824–1833.
4. Abel ED. Glucose transport in the heart. *Front Biosci*. 2004;9:201–215.
5. Brosius FC III, Liu Y, Nguyen N, Sun D, Bartlett J, Schwaiger M. Persistent myocardial ischemia increases GLUT1 glucose transporter expression in both ischemic and non-ischemic heart regions. *J Mol Cell Cardiol*. 1997;29:1675–1685.
6. Tian R, Musi N, D'Agostino J, Hirshman MF, Goodyear LJ. Increased adenosine monophosphate-activated protein kinase activity in rat hearts with pressure-overload hypertrophy. *Circulation*. 2001;104:1664–1669.
7. Opie LH, Sack MN. Metabolic plasticity and the promotion of cardiac protection in ischemia and ischemic preconditioning. *J Mol Cell Cardiol*. 2002;34:1077–1089.
8. Gertz EW, Wisneski JA, Stanley WC, Neese RA. Myocardial substrate utilization during exercise in humans. Dual carbon-labeled carbohydrate isotope experiments. *J Clin Invest*. 1988;82:2017–2025.
9. Liao R, Jain M, Cui L, D'Agostino J, Aiello F, Luptak I, Ngoy S, Mortensen RM, Tian R. Cardiac-specific overexpression of GLUT1 prevents the development of

heart failure attributable to pressure overload in mice. *Circulation*. 2002;106:2125–2131.

10. Luptak I, Yan J, Cui L, Jain M, Liao R, Tian R. Long-term effects of increased glucose entry on mouse hearts during normal aging and ischemic stress. *Circulation*. 2007;116:901–909.
11. Malmberg K, Ryden L. Effect of insulin-glucose infusion on mortality following acute myocardial infarction in patients with diabetes: the diabetes and insulin-glucose infusion in acute myocardial infarction studies. *Semin Thorac Cardiovasc Surg*. 2006;18:326–329.
12. Poornima I, Brown SB, Bhashyam S, Parikh P, Bolukoglu H, Shannon RP. Chronic glucagon-like peptide-1 infusion sustains left ventricular systolic function and prolongs survival in the spontaneously hypertensive, heart failure-prone rat. *Circ Heart Fail*. 2008;1:153–160.
13. Doenst T, Pytel G, Schrepper A, Amorim P, Farber G, Shingu Y, Mohr FW, Schwarzer M. Decreased rates of substrate oxidation ex vivo predict the onset of heart failure and contractile dysfunction in rats with pressure overload. *Cardiovasc Res*. 2010;86:461–470.
14. Bugger H, Schwarzer M, Chen D, Schrepper A, Amorim PA, Schoepe M, Nguyen TD, Mohr FW, Khalimonchuk O, Weimer BC, Doenst T. Proteomic remodelling of mitochondrial oxidative pathways in pressure overload-induced heart failure. *Cardiovasc Res*. 2010;85:376–384.
15. Mazumder PK, O'Neill BT, Roberts MW, Buchanan J, Yun UJ, Cooksey RC, Boudina S, Abel ED. Impaired cardiac efficiency and increased fatty acid oxidation in insulin-resistant ob/ob mouse hearts. *Diabetes*. 2004;53:2366–2374.
16. Riehle C, Wende AR, Zaha VG, Pires KM, Wayment B, Olsen C, Bugger H, Buchanan J, Wang X, Moreira AB, Doenst T, Medina-Gomez G, Litwin SE, Lelliott CJ, Vidal-Puig A, Abel ED. PGC-1beta deficiency accelerates the transition to heart failure in pressure overload hypertrophy. *Circ Res*. 2011;109:783–793.
17. Bricker DK, Taylor EB, Schell JC, Orsak T, Boutron A, Chen YC, Cox JE, Cardon CM, Van Vranken JG, Dephoure N, Redin C, Boudina S, Gygi SP, Brivet M, Thummel CS, Rutter J. A mitochondrial pyruvate carrier required for pyruvate uptake in yeast, Drosophila, and humans. *Science*. 2012;337:96–100.
18. Boudina S, Sena S, O'Neill BT, Tathireddy P, Young ME, Abel ED. Reduced mitochondrial oxidative capacity and increased mitochondrial uncoupling impair myocardial energetics in obesity. *Circulation*. 2005;112:2686–2695.
19. Sena S, Rasmussen IR, Wende AR, McQueen AP, Theobald HA, Wilde N, Pereira RO, Litwin SE, Berger JP, Abel ED. Cardiac hypertrophy caused by peroxisome proliferator-activated receptor-gamma agonist treatment occurs independently of changes in myocardial insulin signaling. *Endocrinology*. 2007;148:6047–6053.
20. Boudina S, Sena S, Theobald H, Sheng X, Wright JJ, Hu XX, Aziz S, Johnson JI, Bugger H, Zaha VG, Abel ED. Mitochondrial energetics in the heart in obesity-related diabetes: direct evidence for increased uncoupled respiration and activation of uncoupling proteins. *Diabetes*. 2007;56:2457–2466.
21. Shende P, Plaisance I, Morandi C, Pellieux C, Berthonneche C, Zorzato F, Krishnan J, Lerch R, Hall MN, Ruegg MA, Pedrazzini T, Brink M. Cardiac raptor ablation impairs adaptive hypertrophy, alters metabolic gene expression, and causes heart failure in mice. *Circulation*. 2011;123:1073–1082.
22. Hu Y, Belke D, Suarez J, Swanson E, Clark R, Hoshijima M, Dillmann WH. Adenovirus-mediated overexpression of O-GlcNAcase improves contractile function in the diabetic heart. *Circ Res*. 2005;96:1006–1013.
23. Lunde IG, Aronsen JM, Kvaloy H, Qvigstad E, Sjaastad I, Tonnessen T, Christensen G, Gronning-Wang LM, Carlson CR. Cardiac O-GlcNAc signaling is increased in hypertrophy and heart failure. *Physiol Genomics*. 2012;44:162–172.
24. Sen S, Kundu BK, Wu HC, Hashmi SS, Guthrie P, Locke LW, Roy RJ, Matherne GP, Berr SS, Terwelp M, Scott B, Carranza S, Frazier OH, Glover DK, Dillmann WH, Gambello MJ, Entman ML, Taegtmeyer H. Glucose regulation of load-induced mTOR signaling and ER stress in mammalian heart. *J Am Heart Assoc*. 2013;2:e004796.
25. Allard MF, Schonekess BO, Henning SL, English DR, Lopaschuk GD. Contribution of oxidative metabolism and glycolysis to ATP production in hypertrophied hearts. *Am J Physiol*. 1994;267:H742–H750.
26. Bishop SP, Altschuld RA. Increased glycolytic metabolism in cardiac hypertrophy and congestive failure. *Am J Physiol*. 1970;218:153–159.
27. Taegtmeyer H, Overturf ML. Effects of moderate hypertension on cardiac function and metabolism in the rabbit. *Hypertension*. 1988;11:416–426.
28. Zhang J, Duncker DJ, Ya X, Zhang Y, Pavek T, Wei H, Merkle H, Ugurbil K, From AH, Bache RJ. Effect of left ventricular hypertrophy secondary to chronic pressure overload on transmural myocardial 2-deoxyglucose uptake. A 31p NMR spectroscopic study. *Circulation*. 1995;92:1274–1283.
29. Eberli FR, Weinberg EO, Grice WN, Horowitz GL, Apstein CS. Protective effect of increased glycolytic substrate against systolic and diastolic dysfunction and increased coronary resistance from prolonged global underperfusion and reperfusion in isolated rabbit hearts perfused with erythrocyte suspensions. *Circ Res*. 1991;68:466–481.
30. Rimbaud S, Garnier A, Ventura-Clapier R. Mitochondrial biogenesis in cardiac pathophysiology. *Pharmacol Rep*. 2009;61:131–138.
31. Moley KH, Mueckler MM. Glucose transport and apoptosis. *Apoptosis*. 2000;5:99–105.
32. Malhotra R, Tyson DG, Sone H, Aoki K, Kumagai AK, Brosius FC III. Glucose uptake and adenoviral mediated GLUT1 infection decrease hypoxia-induced HIF-1alpha levels in cardiac myocytes. *J Mol Cell Cardiol*. 2002;34:1063–1073.
33. Lin Z, Weinberg JM, Malhotra R, Merritt SE, Holzman LB, Brosius FC III. GLUT-1 reduces hypoxia-induced apoptosis and JNK pathway activation. *Am J Physiol Endocrinol Metab*. 2000;278:E958–E966.
34. Morissette MR, Howes AL, Zhang T, Heller Brown J. Upregulation of GLUT1 expression is necessary for hypertrophy and survival of neonatal rat cardiomyocytes. *J Mol Cell Cardiol*. 2003;35:1217–1227.
35. Abel ED, Doenst T. Mitochondrial adaptations to physiological vs pathological cardiac hypertrophy. *Cardiovasc Res*. 2011;90:234–242.
36. Wei H, Bedja D, Koitabashi N, Xing D, Chen J, Fox-Talbot K, Rouf R, Chen S, Steenbergen C, Harmon JW, Dietz HC, Gabrielson KL, Kass DA, Semenza GL. Endothelial expression of hypoxia-inducible factor 1 protects the murine heart and aorta from pressure overload by suppression of tgf-beta signaling. *Proc Natl Acad Sci USA*. 2012;109:E841–E850.
37. Nagle DG, Zhou YD. Natural product-derived small molecule activators of hypoxia-inducible factor-1 (HIF-1). *Curr Pharm Des*. 2006;12:2673–2688.
38. McFate T, Mohyeldin A, Lu H, Thakar J, Henriques J, Halim ND, Wu H, Schell MJ, Tsang TM, Teahan O, Zhou S, Califano JA, Jeoung NH, Harris RA, Verma A. Pyruvate dehydrogenase complex activity controls metabolic and malignant phenotype in cancer cells. *J Biol Chem*. 2008;283:22700–22708.
39. Ago T, Kuroda J, Pain J, Fu C, Li H, Sadoshima J. Upregulation of NOX4 by hypertrophic stimuli promotes apoptosis and mitochondrial dysfunction in cardiac myocytes. *Circ Res*. 2010;106:1253–1264.
40. Kuroda J, Ago T, Matsushima S, Zhai P, Schneider MD, Sadoshima J. Nadph oxidase 4 (NOX4) is a major source of oxidative stress in the failing heart. *Proc Natl Acad Sci USA*. 2010;107:15565–15570.
41. Scortegagna M, Ding K, Oktay Y, Gaur A, Thurmond F, Yan LJ, Marck BT, Matsumoto AM, Shelton JM, Richardson JA, Bennett MJ, Garcia JA. Multiple organ pathology, metabolic abnormalities and impaired homeostasis of reactive oxygen species in Epas1−/− mice. *Nat Genet*. 2003;35:331–340.
42. Lu Z, Xu X, Hu X, Fassett J, Zhu G, Tao Y, Li J, Huang Y, Zhang P, Zhao B, Chen Y. PGC-1 alpha regulates expression of myocardial mitochondrial antioxidants and myocardial oxidative stress after chronic systolic overload. *Antioxid Redox Signal*. 2010;13:1011–1022.
43. Zhang T, Maier LS, Dalton ND, Miyamoto S, Ross J Jr, Bers DM, Brown JH. The deltaC isoform of CaMKII is activated in cardiac hypertrophy and induces dilated cardiomyopathy and heart failure. *Circ Res*. 2003;92:912–919.
44. Maier LS, Zhang T, Chen L, DeSantiago J, Brown JH, Bers DM. Transgenic CaMKIIdeltaC overexpression uniquely alters cardiac myocyte Ca2+ handling: reduced SR Ca2+ load and activated SR Ca2+ release. *Circ Res*. 2003;92:904–911.
45. Lompre AM, Hajjar RJ, Harding SE, Kranias EG, Lohse MJ, Marks AR. Ca2+ cycling and new therapeutic approaches for heart failure. *Circulation*. 2010;121:822–830.
46. MacLennan DH, Kranias EG. Phospholamban: a crucial regulator of cardiac contractility. *Nat Rev Mol Cell Biol*. 2003;4:566–577.
47. Ren J, Gintant GA, Miller RE, Davidoff AJ. High extracellular glucose impairs cardiac E-C coupling in a glycosylation-dependent manner. *Am J Physiol*. 1997;273:H2876–H2883.
48. Razeghi P, Myers TJ, Frazier OH, Taegtmeyer H. Reverse remodeling of the failing human heart with mechanical unloading. Emerging concepts and unanswered questions. *Cardiology*. 2002;98:167–174.
49. Razeghi P, Young ME, Alcorn JL, Moravec CS, Frazier OH, Taegtmeyer H. Metabolic gene expression in fetal and failing human heart. *Circulation*. 2001;104:2923–2931.